AIP | Applied Physics Letters

Dynamic non-reciprocal meta-surfaces with arbitrary phase reconfigurability based on photonic transition in meta-atoms

Yu Shi and Shanhui Fan

Citation: Applied Physics Letters **108**, 021110 (2016); doi: 10.1063/1.4939915
View online: http://dx.doi.org/10.1063/1.4939915
View Table of Contents: http://scitation.aip.org/content/aip/journal/apl/108/2?ver=pdfcov
Published by the AIP Publishing

Dynamic non-reciprocal meta-surfaces with arbitrary phase reconfigurability based on photonic transition in meta-atoms

Yu Shi and Shanhui Fan[a)]
Ginzton Laboratory, Department of Electrical Engineering, Stanford University, Stanford, California 94305, USA

(Received 16 October 2015; accepted 3 January 2016; published online 14 January 2016)

We introduce a distinct class of dynamic non-reciprocal meta-surfaces with arbitrary phase-reconfigurability. This meta-surface consists of an array of meta-atoms, each of which is subject to temporal refractive index modulation, which induces photonic transitions between the states of the meta-atom. We show that arbitrary phase profile for the outgoing wave can be achieved by controlling the phase of the modulation at each meta-atom. Moreover, such dynamic meta-surfaces exhibit non-reciprocal response without the need for magneto-optical effects. The use of photonic transition significantly enhances the tunability and the possible functionalities of meta-surfaces. © *2016 AIP Publishing LLC*. [http://dx.doi.org/10.1063/1.4939915]

The ability to manipulate the phase-front of light waves is central to optical engineering. Traditional optical components rely on the mechanism of gradual phase-accumulation as light propagates inside an optical medium, but such mechanism often results in bulky devices that are thicker than the operating wavelength because the accumulated phase is limited by the permittivity of naturally existing materials.[1,2] To overcome the limitations of traditional optical components, two-dimensional metamaterials, or meta-surfaces, have been recently developed. A meta-surface, consisting of an array of meta-atoms (i.e., subwavelength resonators), can apply abrupt phase-changes for light propagating through the meta-surface.[1–3] By designing the amplitude and phase responses of these meta-atoms to an incident wave, a meta-surface can create an arbitrary phase-gradient along its interface and hence can flexibly shape the out-going wave-front according to the generalized Snell's Law.[3] With specific subwavelength meta-atom designs, ultra-thin meta-surfaces have been used to manipulate the polarization of light,[4–8] steer and focus beams,[3,9] create thin refractive and diffractive optical components,[10–17] and realize special optical physics effects, such as generating vortex beams[18] and optical spin Hall effects.[19,20]

In spite of tremendous recent progresses in meta-surfaces, there are two significant opportunities that have not yet been extensively exploited. First of all, most of these meta-surfaces are constrained by the Lorentz reciprocity theorem. Yet breaking the reciprocity can lead to non-reciprocal meta-surfaces with significant functionalities, such as optical isolation on an ultrathin surface.[21–23] Very recently, Shaltout *et al*. outlined the theoretical formalism for realizing non-reciprocal metasurfaces using time-gradient phase discontinuities,[22] and Hadad *et al*. demonstrated that a non-reciprocal electromagnetic induced transparency can be introduced from a spatio-temporally modulated metasurface with a sinusoidal impedance.[23] Second, in most of the meta-surfaces, the phase responses of the individual meta-atoms are almost entirely fixed by their geometries. While it is possible to tune such phase responses by refractive index tuning, the achievable tunability is rather limited. In particular, it still remains a significant challenge to tune the phase response of an individual meta-atom over the entire range of $[0, 2\pi]$, which is required in order to achieve arbitrary reconfiguration of meta-surfaces.

Here, we propose to create non-reciprocal dynamic meta-surface by exploiting the concept of photonic transition[24–29] and photonic Aharonov-Bohm effects[30,31] as recently proposed theoretically and demonstrated experimentally. Similar to Refs. 22 and 23, our approach breaks reciprocity in a dynamic meta-surface without the use of magneto-optical effect. Unlike Refs. 22 and 23, however, our approach also provides arbitrary phase reconfigurability and hence can lead to a wider range of applications. Consider any optical system with two photonic states at two difference frequencies, undergoing a time-harmonic refractive index modulation. When the frequency of the modulation matches the frequency difference between the two photonic states, a photonic transition occurs between the two states. It has been shown that such a modulation breaks reciprocity. Moreover, the phase of the modulation is imprinted on the amplitudes of the photonic states.[27,30,31] Since the modulation phase is imposed dynamically after the structure has been constructed, it can be arbitrarily set. In this letter, we show that such photonic transition can occur in subwavelength meta-atoms, and an array of such meta-atoms undergoing photonic transitions can function as a non-reciprocal meta-surface with the capability of arbitrary reconfiguration.

To start, we first briefly review the concept of photonic transition in the context of meta-atoms [Fig. 1(a)]. Consider a meta-atom with a time-independent dielectric function $\epsilon_{DC}(\mathbf{r})$, supporting eigenstates $|1\rangle$ and $|2\rangle$ at frequencies ω_1 and ω_2 with amplitudes $a_1(t)$ and $a_2(t)$, respectively. Without loss of generality, we assume $\omega_2 > \omega_1$. We then induce coupling between these two states by applying to the meta-atom a permittivity modulation, as described by a dielectric function

[a)]Author to whom correspondence should be addressed. Electronic mail: shanhui@stanford.edu.

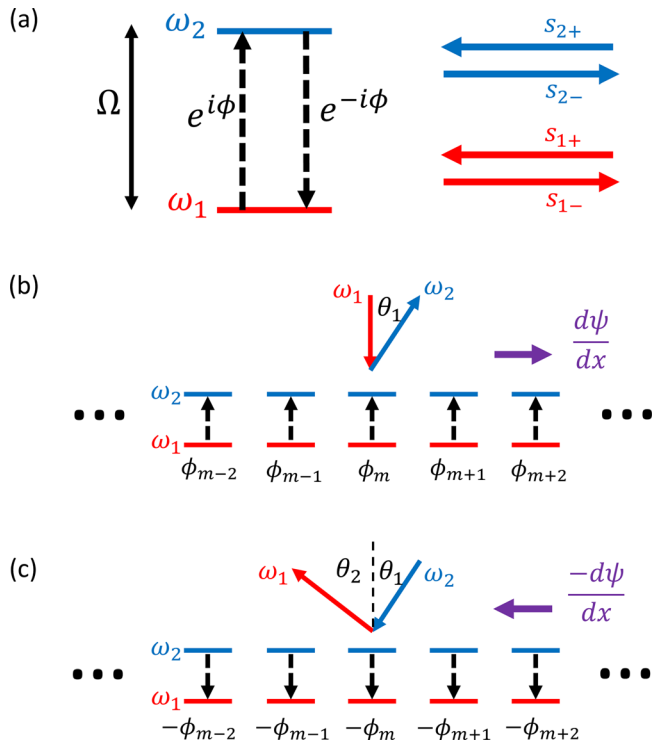

FIG. 1. Design principle of a dynamic meta-surface based on photonic transitions in meta-atoms. (a) Schematic of a meta-atom supporting two resonances and coupling to two external ports. The meta-atom is temporally modulated to induce a photonic transition between the two resonances. (b) Anomalous reflection of a normally incident wave at ω_1 from a meta-surface. The meta-surface consists of an array of meta-atoms, each as shown in (a). The modulation phases of the meta-atoms have a linearly varying profile in space. (c) Anomalous reflection from the same meta-surface with the same spatial modulation phase profile, for an incident wave that is obtained by time-reversing the outgoing wave in (b). Due to the time-reversal symmetry breaking photonic transition, the outgoing wave at ω_1 propagates in a different direction from the normal direction.

$$\epsilon(\mathbf{r}, t) = \epsilon_{DC}(\mathbf{r}) + \delta(\mathbf{r})\cos(\Omega t + \phi), \tag{1}$$

where $\Omega = \omega_2 - \omega_1$ is the modulation frequency chosen to be equal to the frequency difference between the two states, ϕ is the modulation phase, and $\delta(\mathbf{r})$ describes the modulation profile in space. We further assume that the states can couple to external radiation. For the sake of brevity, we consider two input ports and output ports with amplitudes $s_{1\pm}$ at ω_1 and $s_{2\pm}$ at ω_2, where the "+" and "−" subscripts denote input and output waves, respectively [Figure 1(a)]. Using the rotating wave approximation,[27,30] the dynamics of the system can then be described by the temporal coupled-mode equations[32]

$$\begin{aligned}
\dot{a}_1 &= (i\omega_1 - \gamma_1)a_1 + i\kappa e^{-i\Omega t}e^{-i\phi}a_2 + k_1 s_{1+},\\
\dot{a}_2 &= (i\omega_2 - \gamma_2)a_2 + i\kappa e^{+i\Omega t}e^{+i\phi}a_1 + k_2 s_{2+},\\
s_{1-} &= c_1 s_{1+} + k_1 a_1,\\
s_{2-} &= c_2 s_{2+} + k_2 a_2,
\end{aligned} \tag{2}$$

where γ_n denotes the amplitude decay rate of the n-th modes, κ represents the coupling strength between the two modes induced by the permittivity modulation, k_n characterizes the coupling strength between ports $s_{n\pm}$ and mode a_n, and c_n represents the direct scattering from port s_{n+} to s_{n-} that does not go through the meta-atom. To extract the steady-state behavior, we consider the excitation of the system at frequency ω such that $a_1(t) = \tilde{a}_1 e^{i\omega t}$ and $a_2(t) = \tilde{a}_2 e^{i\omega t}$, where $\tilde{a}_1$ and $\tilde{a}_2$ are the modal amplitudes for states $|1\rangle$ and $|2\rangle$, respectively. By substituting $A_1(t) = a_1(t)e^{\frac{i\Omega t}{2}} = \tilde{a}_1 e^{i\left(\omega+\frac{\Omega}{2}\right)t}$, $A_2(t) = a_2(t)e^{\frac{-i\Omega t}{2}} = \tilde{a}_2 e^{i\left(\omega-\frac{\Omega}{2}\right)t}$, $s_{1\pm}(t) = S_{1\pm}(t)e^{-\frac{i\Omega t}{2}}$, and $s_{2\pm}(t) = S_{2\pm}(t)e^{\frac{i\Omega t}{2}}$, we obtain the following steady-state solutions:

$$\begin{aligned}
A_1 &= \frac{ik_2\kappa e^{-i\phi}}{D}S_{2+} + \frac{k_1\left(i(\omega-\omega_0)+\gamma_2\right)}{D}S_{1+},\\
A_2 &= \frac{ik_1\kappa e^{i\phi}}{D}S_{1+} + \frac{k_2\left(i(\omega-\omega_0)+\gamma_1\right)}{D}S_{2+},\\
S_{1-} &= \left(c_1 + \frac{{k_1}^2\left(i(\omega-\omega_0)+\gamma_2\right)}{D}\right)S_{1+} + \frac{ik_1k_2\kappa e^{-i\phi}}{D}S_{2+},\\
S_{2-} &= \left(c_2 + \frac{{k_2}^2\left(i(\omega-\omega_0)+\gamma_1\right)}{D}\right)S_{2+} + \frac{ik_1k_2\kappa e^{i\phi}}{D}S_{1+},
\end{aligned} \tag{3}$$

where $D = (i(\omega-\omega_0)+\gamma_1)\ (i(\omega-\omega_0)+\gamma_2) + \kappa^2$ and $\omega_0 = (\omega_1+\omega_2)/2$. From Eq. (3), we can readily see that when $S_{1+} = 0$, S_{1-} at ω_1 can be generated from S_{2+} at ω_2 as

$$S_{1-} = \frac{ik_1k_2\kappa e^{-i\phi}}{D}S_{2+}. \tag{4a}$$

And when $S_{2+} = 0$, S_{2-} at ω_2 can be generated from S_{1+} at ω_1 as

$$S_{2-} = \frac{ik_1k_2\kappa e^{i\phi}}{D}S_{1+}. \tag{4b}$$

Therefore, upon the transition from $|1\rangle$ to $|2\rangle$ that is upward in frequency, the wave emitted to port s_{2-} would carry a phase ϕ, whereas during a downward transition from $|2\rangle$ to $|1\rangle$, the same modulation prescribes a phase $-\phi$ to waves emitted at port s_{1-}. Such a direction-dependent phase in photonic transition is the essence of the photonic Aharonov-Bohm effect and can be used to break reciprocity.[30,31] The results in Eq. (4) show that the photonic Aharonov-Bohm effect can be achieved in the steady-state response of a meta-atom undergoing refractive index modulation. The conversion efficiency $\eta = |\frac{k_1k_2\kappa}{D}|^2$ can reach unity in a lossless system, provided that $\kappa^2 = \gamma_1\gamma_2$. This result can be simply obtained since with the transformation as discussed above, the system as described by Eq. (2) in fact maps exactly to the static coupled-resonator system as discussed in Ref. 33. The significance of the present work however is the effect of modulation phase, which is unique in dynamic systems and hence is the main focus of our paper.

Having discussed the photonic transition in an individual meta-atom, we now consider an array of such meta-atoms, each undergoing photonic-transitions [Fig. 1(b)]. Since the refractive index modulation of each meta-atom is imposed dynamically after the structure is constructed, we may independently control the modulation phase on each meta-atom and hence can create arbitrary phase profiles on the meta-surface. Assume that a plane wave with a frequency ω_1 is incident on the meta-surface with an angle of incidence θ_i. The outgoing wave at ω_2 picks up a discrete phase-profile $\psi(x)$

$$\psi(m\Lambda) = \phi_m, \tag{5}$$

where Λ is the spacing between the meta-atoms, and ϕ_m is the modulation phase at the m-th meta-atom. For a meta-surface, we assume that Λ is much less than the wavelength, so that the phase profile $\psi(x)$ can be approximated as continuous. The outgoing wave at ω_2 now follows the generalized Snell's Law,[22] namely,

$$k_o \sin\theta_o = k_i \sin\theta_i + \frac{\partial\psi}{\partial x}, \tag{6}$$

where k_i, k_o are the incident and outgoing waves' momenta, θ_o is the angle that characterizes the direction of the outgoing wave, and $\frac{\partial\psi}{\partial x}$ quantifies the gradient of the phase profile as induced by the photonic-transitions in the meta-atoms. With a constant phase gradient $\frac{\partial\psi}{\partial x}$, an outgoing wave at ω_2 can experience anomalous reflection and refraction with respect to the incident wave at ω_1.[2,22] Moreover, a spatially variant $\frac{\partial\psi}{\partial x}$ provides an arbitrary phase-front for the outgoing wave at ω_2 and can be used for focusing and other beam-shaping functionalities.

Such a meta-surface undergoing dynamic modulation has a non-reciprocal response. As an illustration, consider the situation as shown in Figure 1(b), where a plane wave at ω_1 is normally incident upon the meta-surface. We choose a constant phase gradient such that the outgoing wave at ω_2 exhibits anomalous reflection with respect to incoming wave, with a parallel wavevector $k_2 \sin\theta_2 = \frac{\partial\psi}{\partial x}$. Now, we consider the time-reversed situation as shown in Figure 1(c), where an incoming beam at ω_2, at a direction that corresponds to the time-reversal of the outgoing beam in Figure 1(b), is incident upon the meta-surface undergoing the same modulation. The outgoing beam at ω_1 in this time-reversed situation will not be at the normal direction, and instead will have a parallel wave-vector of $k_1 \sin\theta_1 = -2\frac{\partial\psi}{\partial x}$ [Fig. 1(c)]. This result arises due to the extra minus sign when the photon undergoes a downward transition. Therefore, we see in this illustration that the meta-surface indeed breaks time-reversal symmetry and reciprocity.

To verify our theoretical predictions, we perform finite-difference time-domain (FDTD) simulations with a reflective meta-surface formed by an array of independently modulated meta-atoms on top of a gold substrate. As a proof of principle, we consider only the transverse-electric (TE) polarization (i.e., the only field components that are non-zero are E_z, H_x, and H_y). The meta-atom consists of a gold patch cover and two gold side walls mounted on the gold substrate [Fig. 2(a)]. The cover and the side walls are 120 nm wide, with the cover being 200 nm long. The dielectric medium enclosed in the meta-atom is chosen as silicon, and it has a dimension of 600 nm in height and 440 nm in width. The sidewalls ensure that the modes of a meta-atom are sufficiently contained in itself and do not interfere with the modes of neighboring meta-atoms. In the FDTD simulations, the spatial resolution in the x and y directions is 40 nm, and the time step 0.067 fs. Perfectly matched absorbing layers are used to surround the simulation domain.[34] Dispersive FDTD update equations[35] are used to account for material dispersion in gold and silicon. The frequency-dependent dielectric constants of gold, including both the real and imaginary parts, are obtained from Rakic,[36] and we fit them with a Drude model. For silicon, we ensure that our fit agrees well with the data in Li[37] in the frequency range of our interest.

A single resonator described above can support an even mode $|1\rangle$ at $\lambda_1 = 2790$ nm and an odd mode $|2\rangle$ at $\lambda_2 = 1950$ nm, with their respective modal profiles shown in Figure 2(b) as obtained from the FDTD simulations. Here, the even and odd symmetries are defined with respect to a mirror plane parallel to the x-axis; the symmetries are approximate since the mirror plane is not an exact one. The dimensions of the meta-atom are far smaller than the resonant wavelengths, and hence, the radiation patterns for the two resonator modes are both nearly cylindrical. Having such nearly identical radiation patterns for these two modes ensures that incoming far-field radiation couples to these two modes with comparable strengths. In the absence of dynamic permittivity modulation, these two modes exist independently.

We perform FDTD simulations on a modulated meta-surface constructed from an array of 13 meta-atoms as described above. The array has a period of $\Lambda = 800$ nm. For each meta-atom, the permittivity modulation is applied uniformly in the region as represented by the dashed rectangle in Figure 2(c), and has the form $\delta\cos(\Omega t + \phi)$, where

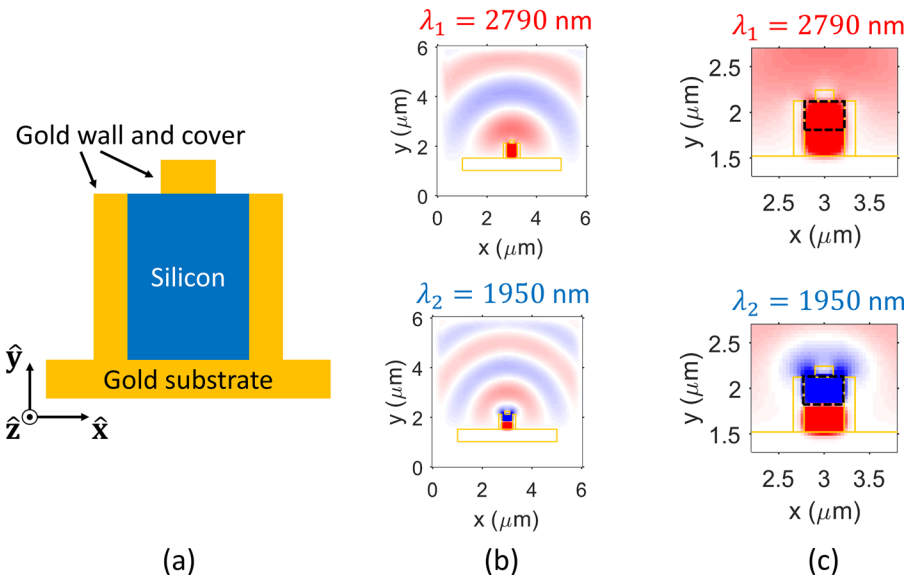

FIG. 2. Meta-atom structure and modes. (a) The geometry of a single meta-atom. (b) The modal profiles of the resonator at $\lambda_1 = 2790$ nm and $\lambda_2 = 1950$ nm. Both modes have a cylindrical far-field radiation pattern. (c) The zoomed-in view of the modal profile. The boxed region is the dielectric region that undergoes dynamic modulation.

$\delta = 0.1$ is the strength of modulation used in the simulation, $\Omega = 46.3$ THz, and ϕ is specified for each individual meta-atom separately. The modulation strength was chosen such that a noticeable mode conversion can be observed without making the effort to maximize the conversion efficiency. We apply the total-field scattered-field algorithm to simulate an incident wave that has infinite spatial extent in the direction transverse to propagation.[35] In the first set of simulations (Figure 3), we send in normally incident plane wave at $\lambda_1 = 2790$ nm so that every meta-atom is equally excited with the same phase [Fig. 3(a)]. Concurrently, we modulate each meta-atom as described above. In Figures 3(b)–3(d), we consider three different phase profiles. To focus the wave at $\lambda_2 = 1950$ nm along the normal axis of the meta-surface, we may choose a symmetric modulation profile of $\{\phi_m\} = k_2\sqrt{h^2 + (m\Lambda)^2}$, where $k_2 = \frac{2\pi}{\lambda_2}$, h is the focal height, and m is an integer that varies from -6 to 6, with $m = 0$ corresponding to the meta-atom at the center of the array. In Figure 3(b), we choose $h = 8\,\mu$m and indeed observe that such a modulation phase enables on-axis focusing of the outgoing wave at 8 μm above the meta-surface. In Figure 3(c), we choose another modulation profile with $h = 5\,\mu$m. We see that the focal point remains along the same axis but is now closer to the meta-surface as compared to the case in Figure 3(b). One can therefore control the position of the focal point by changing the modulation phase profile. Finally, the same structure can enable off-axis focusing as well, with a modulation profile of $\{\phi_m\} = k_2\sqrt{h^2+(x-m\Lambda)^2}$, where x is the horizontal shift in the focal point. We show this in Figure 3(d) by choosing h=7μm and x=3μm. The simulations here demonstrate the capability for dynamically reconfiguring the meta-surface in order to flexibly tailor the phase-front of the outgoing light through the control of modulation phases.

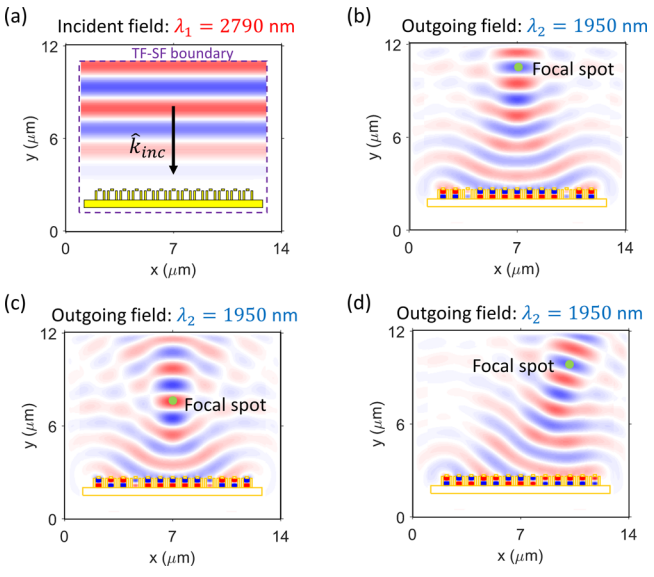

FIG. 3. Dynamic focusing from the meta-surface, as simulated using the total-field scattered-field formalism in FDTD. (a) Normally incident plane-wave at λ_1. The dashed line represents the boundary between the total field and the scattered field region. (b)–(d) By varying the modulation phase profile along the meta-surface interface, the outgoing wave at λ_2 can be focused at various focal points, either on or off axis.

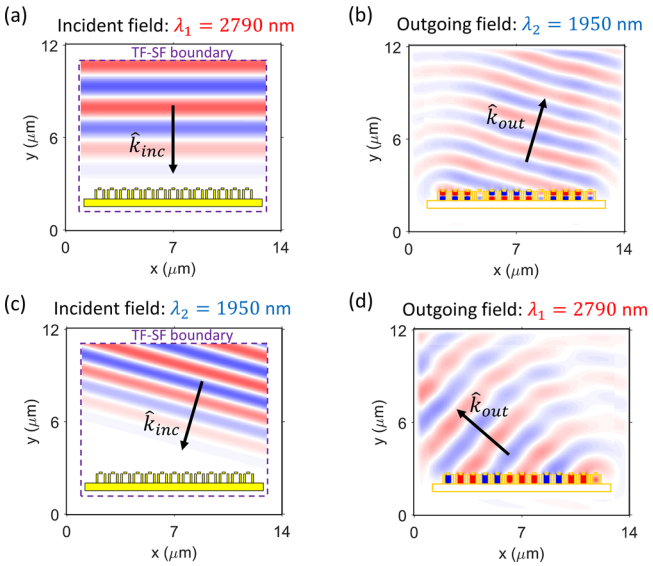

FIG. 4. Demonstration of non-reciprocal response from the meta-surface as simulated using the total-field scattered-field formalism in FDTD. (a) Normally incident plane-wave at λ_1. The dashed line represents the boundary between the total field region and the scattered field region. (b) Outgoing wave at λ_2 as generated by the incident wave in (a). The outgoing wave is approximately a plane-wave propagating at an angle of 15° with respect to the direction normal to the meta-surface due to the linearly varying modulation phase profile imposed on the meta-surface. (c) The incident wave is now switched to a plane-wave that is the time-reversal of the plane-wave of (b). (d) In response to the incident wave in (c), the outgoing wave at λ_1 propagates at an angle of around 48° with respect to normal.

We then perform simulations on the same meta-surface to demonstrate non-reciprocity. Here, we apply a modulation phase profile $\{\phi_m\}$ to the meta-atoms that corresponds to a constant phase-gradient $\frac{\partial\psi}{\partial x} = 0.834\,\mu\text{m}^{-1}$ on the meta-surface. As we send in a normally incident plane wave at $\lambda_1 = 2790$ nm [Fig. 4(a)], in consistency with the calculations using the generalized Snell's Law in Eq. (6), the outgoing plane wave at $\lambda_2 = 1950$ nm is deflected to an angle of 15° as shown in Figure 4(b). In the time-reversed scenario, when we send in a plane wave at $\lambda_2 = 1950$ nm back onto the meta-surface at an incident angle of $-15°$ [Fig. 4(c)], the down-conversion from λ_2 to λ_1 implies that the phase-gradient picked up by λ_1 is in fact $-\frac{\partial\psi}{\partial x} = -0.834\,\mu\text{m}^{-1}$, which, according to the generalized Snell's Law in Eq. (6), would deflect λ_1 to an output angle of $-47.8°$, as we indeed observe in the simulation [Fig. 4(d)]. The FDTD simulations provide strong evidence that our meta-surface breaks time-reversal symmetry. Such non-reciprocal meta-surface design allows it to potentially be used for optical isolation or circulation purposes, which are important in laser feedback prevention, optical computing, and optical communication systems. Since our meta-surface has a linear response with respect to the incoming wave, its non-reciprocity does not suffer from the dynamic reciprocity considerations that constrain the performance of nonlinear non-reciprocal structures.[38]

In the simulation above, both the strength ($\frac{\delta}{\epsilon_{DC}} \sim 10^{-2}$) and the frequency ($\Omega \sim 10$ THz) of the modulation are chosen for the ease of simulation. The agreement of the simulation with the theoretical predictions on the properties of the outgoing beam provides a validation of the physics as

illustrated by the coupled mode theory equations. In principle, the high-frequency modulation that we assumed can be achieved using $\chi^{(2)}$ effect such as sum-frequency generation. Moreover, experimentally, one can design meta-atom structures in which the difference in modal frequencies is in the MHz-GHz range, and induces photonic transitions with either electro-optic[29] or acousto-optic effects.[31] In either case, the strength of modulation ($\frac{\delta}{\epsilon_{DC}} \sim 10^{-4}$) will be far weaker than what we have assumed in the simulation. Since the coupled-mode theory is a perturbation theory with respect to the modulation strength, we expect that the coupled-mode theory formalism, and hence the physics concept as described above, should be applicable for such a dynamic meta-surface undergoing electro-optic or acousto-optic modulations.

In summary, we introduce a class of dynamic non-reciprocal meta-surface structures with arbitrary phase reconfigurability, where the phase profile arises from photonic transition in individual meta-atoms. Such a dynamic meta-surface provides arbitrary phase tunability, as well as non-reciprocity, and should prove to be an important step forward to the development of ultra-thin elements for the control of optical and electromagnetic waves.

This work was supported by Samsung Electronics.

[1]A. Kildishev, A. Boltasseva, and V. Shalaev, "Planar photonics with meta-surfaces," Science **339**, 1232009 (2013).
[2]N. Yu and F. Capasso, "Flat optics with designer metasurfaces," Nat. Mater. **13**, 139–150 (2014).
[3]N. Yu, P. Genevet, M. A. Kats, F. Aieta, J. Tetienne, F. Capasso, and Z. Gaburro, "Light propagation with phase discontinuities-generalized laws of reflection and refraction," Science **334**, 333–337 (2011).
[4]Y. Zhao and A. Alu, "Manipulating light polarization with ultrathin plasmonic metasurfaces," Phys. Rev. B **84**, 205428 (2011).
[5]S. Prosvirnin and N. Zheludev, "Polarization effects in the diffraction of light by a planar chiral structure," Phys. Rev. E **71**, 037603 (2005).
[6]S. Prosvirnin and N. Zheludev, "Analysis of polarization transformations by a planar chiral array of complex-shaped particles," J. Opt. A: Pure Appl. Opt. **11**, 074002 (2009).
[7]A. Papakostas, A. Potts, D. M. Bagnall, S. L. Prosvirnin, H. J. Coles, and N. I. Zheludev, "Optical manifestations of planar chirality," Phys. Rev. Lett. **90**, 107404 (2003).
[8]N. Yu, F. Aieta, P. Genevet, M. A. Kats, Z. Gaburro, and F. Capasso, "A broadband, background-free quarter-wave plate based on plasmonic metasurfaces," Nano Lett. **12**, 6328–6333 (2012).
[9]D. Pozar, S. Targonski, and H. D. Syrigos, "Design of millimeter wave microstrip reflectarrays," IEEE Trans. Antennas Propag. **45**, 287–297 (1997).
[10]Z. Bomzon, G. Biener, V. Kleiner, and E. Hasman, "Space-variant Pancharatnam–Berry phase optical elements with computer-generated subwavelength gratings," Opt. Lett. **27**, 1141–1143 (2002).
[11]L. Verslegers, P. B. Catrysse, Z. Yu, J. White, E. S. Barnard, M. L. Brongersma, and S. Fan, "Plane lenses based on nanoscale slit arrays in a metallic film," Nano Lett. **9**, 235–238 (2009).
[12]F. Aieta, P. Genevet, M. A. Kats, N. Yu, R. Blanchard, Z. Gaburro, and F. Capasso, "Aberration-free ultra-thin flat lenses and axicons at telecom wavelengths based on plasmonic metasurfaces," Nano Lett. **12**, 4932–4936 (2012).
[13]X. Ni, N. Emani, A. Kildishev, A. Boltasseva, and V. Shalaev, "Broadband light bending with plasmonic nanoantennas," Science **335**, 427 (2012).
[14]D. Lin, P. Fan, E. Hasman, and M. Brongersma, "Dielectric gradient metasurface optical elements," Science **345**, 298–302 (2014).
[15]F. Aieta, P. Genevet, N. Yu, M. A. Kats, Z. Gaburro, and F. Capasso, "Out-of-plane reflection and refraction of light by anisotropic optical antenna metasurfaces with phase discontinuities," Nano Lett. **12**, 1702–1706 (2012).
[16]H. Ee, J. Kang, M. Brongersma, and M. Seo, "Shape-dependent light scattering properties of subwavelength silicon nanoblocks," Nano Lett. **15**, 1759–1765 (2015).
[17]X. Ni, S. Ishii, A. Kildishev, and V. Shalaev, "Ultra-thin, planar, Babinet-inverted plasmonic metalenses," Light: Sci. Appl. **2**, e72 (2013).
[18]P. Genevet, N. Yu, F. Aieta, J. Lin, M. A. Kats, R. Blanchard, M. O. Scully, Z. Gaburro, and F. Capasso, "Ultra-thin plasmonic optical vortex plate based on phase discontinuities," Appl. Phys. Lett. **100**, 013101 (2012).
[19]N. Shitrit, I. Bretner, Y. Gorodetski, V. Kleiner, and E. Hasman, "Optical spin Hall effects in plasmonic chains," Nano Lett. **11**, 2038–2042 (2011).
[20]X. Yin, Z. Ye, J. Rho, Y. Wang, and X. Zhang, "Photonic spin hall effect at metasurfaces," Science **339**, 1405–1407 (2013).
[21]A. Mahmoud, A. Davoyan, and N. Engheta, "All-passive nonreciprocal metastructure," Nat. Commun. **6**, 8359 (2015).
[22]A. Shaltout, A. Kildishev, and V. Shalaev, "Time-varying metasurfaces and Lorentz non-reciprocity," Opt. Mater. Express **5**, 2459–2467 (2015).
[23]Y. Hadad, D. Sounas, and A. Alu, "Space-time gradient metasurfaces," Phys. Rev. Lett. B **92**, 100304 (2015).
[24]J. Winn, S. Fan, D. Joannopoulos, and E. Ippen, "Interband transitions in photonic crystals," Phys. Rev. B **59**, 1551 (1999).
[25]P. Dong, S. F. Preble, J. T. Robinson, S. Manipatruni, and M. Lipson, "Inducing photonic transitions between discrete modes in a silicon optical microcavity," Phys. Rev. Lett. **100**, 033904 (2008).
[26]Z. Yu and S. Fan, "Complete optical isolation created by indirect interband photonic transitions," Nat. Photonics **3**, 91–94 (2009).
[27]K. Fang, Z. Yu, and S. Fan, "Realizing effective magnetic field for photons by controlling the phase of dynamic modulation," Nat. Photonics **6**, 782–787 (2012).
[28]M. C. Munoz, A. Y. Petrov, L. O'Faolian, J. Li, T. F. Krauss, and M. Eich, "Optically induced indirect photonic transitions in a slow light photonic crystal waveguide," Phys. Rev. Lett. **112**, 053904 (2014).
[29]H. Lira, Z. Yu, S. Fan, and M. Lipson, "Electrically driven non-reciprocity induced by interband photonic transition on a silicon chip," Phys. Rev. Lett. **109**, 033901 (2012).
[30]K. Fang, Z. Yu, and S. Fan, "Photonic Aharonov-Bohm effect based on dynamic modulation," Phys. Rev. Lett. **108**, 153901 (2012).
[31]E. Li, B. J. Eggleton, K. Fang, and S. Fan, "Photonic Aharonov-Bohm effect in photon-phonon interactions," Nat. Commun. **5**, 3225 (2014).
[32]W. Suh, Z. Wang, and S. Fan, "Temporal coupled-mode theory and the presence of non-orthogonal modes in lossless multimode cavities," IEEE J. Quantum Electron. **40**, 1511–1518 (2004).
[33]X. Yu, T. Skauli, B. Skauli, S. Sandhu, P. Catrysse, and S. Fan, "Wireless power transfer in the presence of metallic plates: Experimental results," AIP Adv. **3**, 062102 (2013).
[34]J. P. Berenger, "A perfectly matched layer for the absorption of electromagnetic waves," J. Comput. Phys. **114**, 185–200 (1994).
[35]A. Taflove and S. Hagness, *Computational Electrodynamics: The Finite-Difference Time-Domain Method, Third ed.* (Artech House, 2005).
[36]A. D. Rakić, A. B. Djurišic, J. M. Elazar, and M. L. Majewski, "Optical properties of metallic films for vertical-cavity optoelectronic devices," Appl. Opt. **37**, 5271–5283 (1998).
[37]H. H. Li, "Refractive index of silicon and germanium and its wavelength and temperature derivatives," J. Phys. Chem. Ref. Data **9**, 561–658 (1980).
[38]Y. Shi, Z. Yu, and S. Fan, "Limitations of nonlinear optical isolators due to dynamic reciprocity," Nat. Photonics **9**, 388–392 (2015).